# Shell model description of zirconium isotopes

K. Sieja,[1,2] F. Nowacki,[3] K. Langanke,[2,4] and G. Martínez-Pinedo[1]

[1]*GSI-Helmholtzzentrum für Schwerionenforschung mbH., Planckstrasse 1, D-64-220 Darmstadt, Germany*

[2]*Institut für Kernphysik, Technische Universität Darmstadt, D-64289 Darmstadt, Germany*

[3]*Institute Pluridisciplinaire Hubert Curien, 23 rue du Loess, Strasbourg, France*

[4]*Frankfurt Institute for Advanced Studies, D-60438 Frankfurt am Main, Germany*

(Received 20 March 2009; published 10 June 2009)

We calculate the low-lying spectra and several high-spin states of zirconium isotopes ($Z = 40$) with neutron numbers from $N = 50$ to $N = 58$ using a large valence space with the $^{78}$Ni inert core, which *a priori* allows one to study the interplay between spherical and deformed configurations, necessary for the description of nuclides in this part of the nuclear chart. The effective interaction is derived by monopole corrections of the realistic $G$ matrix. We reproduce essential nuclear properties, such as subshell closures in $^{96}$Zr and $^{98}$Zr. The spherical-to-deformed shape transition in $^{100}$Zr is addressed as well.

DOI: 10.1103/PhysRevC.79.064310 PACS number(s): 21.60.Cs, 21.10.−k, 27.60.+j

## I. INTRODUCTION

The Zr isotopes between $N = 50$ and $N = 62$ undergo a clear and smooth shape transition with increasing neutron number, from the spherical structure of $^{90-98}$Zr to a rotor in $^{102}$Zr [1–4]. The lightest stable isotope, $^{90}$Zr, lies at the $N = 50$ shell closure. The heaviest stable isotope, $^{96}$Zr, is already very close to the region of deformation, but a large gap between the ground state and the first excited $2^+$ state of 1751 keV suggests a subshell closure. Another interesting feature is that this nucleus is one of the few that have a $0^+$ as their first excited state. Similar spherical structure pertains in $^{98}$Zr; however, the excitation energy of the first excited $0^+$ level drops dramatically to roughly half the value observed in $^{96}$Zr. Spherical-to deformed transition takes place when going from 58 to 60 neutrons, thus when the $\nu g_{7/2}$ orbital is being filled. This abrupt structure change has long been recognized [5] in terms of the strong isoscalar proton-neutron interaction between particles occupying the $g_{9/2}$-$g_{7/2}$ spin-orbit partners. On the edge of this phenomenon are the nuclei with $N = 59$ in which deformed bands have been observed [6,7]. It seems that an important issue for the appearance of the deformation around $A = 100$ and $Z \leqslant 40$ may be the presence of the neutron $g_{9/2}$ extruder: the $9/2^+$ isomers detected in $^{97}$Sr, $^{99}$Zr, and $^{101}$Zr were interpreted as one-neutron hole excitations, and strong ($\beta \sim 0.4$) deformation was deduced for the neutron $9/2^+$ bands (see Ref. [7] and references therein). From the theoretical point of view, understanding the mechanism responsible for the deformation onset in mass 100 is an essential issue for a proper evaluation of the double-$\beta$ nuclear matrix elements for $^{96}$Zr and $^{100}$Mo emitters, where the differences in deformation between parent and daughter nuclei may have substantial impact on the calculated values.

Such dramatic shape changes like those in the zirconium chain are a challenge for any theoretical model, thus the shape transitions in the heavy-Zr region have been calculated by many authors (see e.g., Refs. [8–10] and references cited therein). In most cases, the calculations show large prolate deformations in Sr, Mo, and Zr nuclei with $N \geqslant 60$ (a shape transition appears as well in the neighboring Sr and Mo isotopic chains); however, the details of the transitions are predicted differently and are very sensitive to the adopted model and parametrization, e.g., the relativistic mean-field (RMF) theory with the NL1 force reproduces accurately the deformation changes along the chain, which is no longer the case of RMF with the NL-SH force which predicts a deformed ground state already in $^{94}$Zr [10]. The Skyrme Hartree-Fock models face similar difficulties, e.g., calculations with the SIII force results in prolate deformed ground states starting in $^{94}$Zr [11], while the recent Skyrme-Hartree-Fock-Bogoliubov (HFB14) calculations with the BSk14 parametrization give oblate solutions from $^{94}$Zr to $^{98}$Zr [12]. The deformation parameters along the chain obtained in the commonly used Finite Range Droplet Model (FRDM) [13] do not match the experimental values either. An accurate reproduction of the experimental $B(E2)$ values in Zr chain, i.e., of the deformation parameters, was found in the framework of the interacting boson model (IBM) in Ref. [14].

In the shell model (SM) framework, the shape transition of Zr isotopes was studied by Federman and Pittel [5] using a modest valence space with a $^{94}$Sr core, tractable in SM calculations of that time. In this model, the authors pointed out that in this or other regions of nuclei, the strong isoscalar $T = 0$ part of the proton-neutron interaction may break pairing correlations and hence induce nuclear deformation. However, in Ref. [5] no $B(E2)$ values were calculated, and the deformation was concluded only on the basis of the systematics of the first excited $2^+$ states.

Recently, zirconium isotopes have been studied in Ref. [15] using an inert core of $^{88}$Sr. The authors managed to provide a $G$-matrix-based effective interaction of a satisfying quality as far as $^{91}$Zr–$^{97}$Zr were concerned. For $^{98}$Zr, however, they failed badly to obtain a reasonable agreement with experimental data in the considered valence space.

In this paper, we perform for the first time a SM study of Zr isotopes in an extended model space ($1f_{5/2}$, $2p_{1/2}$, $2p_{3/2}$, $1g_{9/2}$) for protons and ($2d_{5/2}$, $3s_{1/2}$, $2d_{3/2}$, $1g_{7/2}$, $1h_{11/2}$) for neutrons, dubbed hereafter $\pi(r3-g)$, $\nu(r4-h)$. One should notice that no spurious center-of-mass excitations can occur in this valence space, since $J^\pi T = 1^-0$ excitations

 

are not possible. However, two other difficulties arises in the present shell model calculations: first, the dimensions of the full configurational space overcome in general the present computational possibilities, and we have to apply and study different truncation schemes. Second, a reliable effective interaction for this valence space has to be established. To solve this problem, we follow here the procedure to correct the monopole part of the effective interaction to ensure a proper evolution of the single-particle fields. The main task consists in constraining the proton-neutron part. For higher numbers of protons, the shell evolution from $^{91}$Zr to $^{101}$Sn is well known, with the exception of the location of the $\nu h_{11/2}$ orbital beyond $N = 52$, where it is not yet experimentally established. Thus, it is of special interest to investigate theoretically high-spin states that involve excitations to the $h_{11/2}$ orbital, e.g., $[\pi(g_{9/2}) \otimes \nu(g_{7/2}h_{11/2})]$-type of couplings that were detected in several nuclei. Here we refer to isomeric states in Zr isotopes to locate the $h_{11/2}$ centroid and to test the $V_{h_{11/2}\text{-}g_{9/2}}$ proton-neutron part of the effective interaction. In the higher part of the proton shell, the cross-shell interaction is constrained by extending our calculations of low-spin states and electric transitions up to the neutron number $N = 60$ to study the shape change along the chain.

The paper is organized as follows. In the next section we describe briefly the theoretical framework, i.e., the method used to derive the effective interaction and some calculational details. In Sec. III, we show and discuss the results for low-lying states in even and odd zirconium isotopes. Then we discuss the calculations for the known high-spin isomers (III C) and $B(E2)$ transition rates (III D). We also calculate several magnetic properties in $^{92,94}$Zr, where the so-called mixed symmetry states were observed (III E). Finally, we address the problem of the rapid shape change that takes place in $^{100}$Zr (III F). Concluding remarks are collected in Sec. IV.

## II. SHELL MODEL CALCULATIONS

The model space for protons used in the present work was discussed already in Ref. [16]. The effective proton-proton interaction was found by fitting the two-body matrix elements to the available experimental data, namely, for Ni isotopes with $A = 57$–$78$ and $N = 50$ isotones ($^{70}$Cu–$^{100}$Sn). The starting point for the adjusting procedure was a realistic $NN$ interaction based on the Bonn-C potential. Similarly, we have employed the neutron-neutron interaction based on the CD-Bonn potential, previously used in the calculations in the tin region [17], supplemented by a proton-neutron Hamiltonian also obtained from the CD-Bonn. The proton-neutron effective Hamiltonian was corrected in its monopole part to ensure a correct propagation of the single-particle states between $^{79}$Ni and $^{91}$Zr [$\pi(r3)$–$\nu(r4 - h)$ monopoles] and between $^{91}$Zr and $^{101}$Sn [$\pi(g_{9/2})$–$\nu(r4 - h)$ monopoles]. For single-particle levels in $^{101}$Sn, we used the extrapolations of Ref. [18]. Similarly, monopole corrections were applied to the neutron-neutron interaction to reproduce the basic spectroscopy along the tin chain. We show how the proton shells for $Z = 40$ evolve when filling subsequent neutron orbitals in Fig. 1, where the effective single-particle energies (ESPE) [19] calculated with our interaction are traced. The $N = 51$ ESPE for $Z = 28$–$50$ are depicted in Fig. 2.

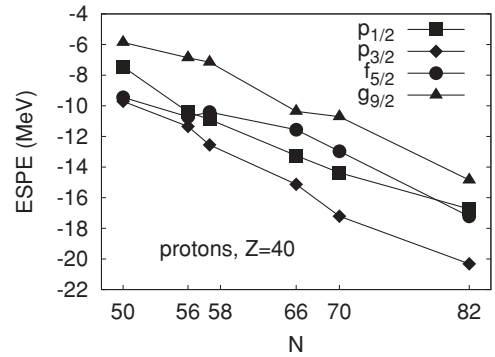


FIG. 1. Proton effective single-particle energies for zirconium isotopes.

The results shown in this work were obtained using the coupled-basis shell-model code NATHAN [20] and the m-scheme code ANTOINE [21]. For $^{90}$Zr–$^{92}$Zr, nontruncated calculations were performed. For larger systems, one needs to use different truncation schemes to reduce the dimensionalities. It is more effective to treat the odd nuclei in the m-scheme and consider particle-hole (p-h) excitations with respect to the $\pi p_{1/2}$ and $\nu d_{5/2}$ shell closures. The even-even nuclei were studied in the coupled scheme with a truncation in seniority. In both cases, we restricted the excitations to the $h_{11/2}$ orbital to maximally 4 particles. The population of this orbital for low-spin states is small (see occupations in Sec. III), thus the additional constraint does not affect the final results considerably. We pursued the calculations up to seniority 8 with NATHAN or up to 8p-8h excitations with ANTOINE. The maximal dimensions considered in this work have been $12 \times 10^9$ for the ground state of $^{97}$Zr in the m-scheme and $9 \times 10^7$ to calculate the $5^-$ state in $^{98}$Zr using the coupled basis. In all studied cases, we reached the convergence of the calculated excitation energies and transition rates. The calculations in which other truncations schemes were used are discussed separately in the text.

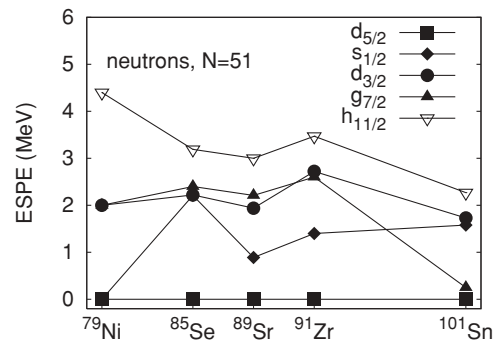


FIG. 2. Evolution of $N = 51$ effective single-particle energies between Ni and Sn.

## III. RESULTS

### A. Odd isotopes

The results of our calculations for odd zirconium isotopes are presented in Figs. 3–6 in comparison with experimental data [1,22,23]. In addition, the SM results from Ref. [15] calculated with the $^{88}$Sr core are shown.

Let us start the discussion with the spectrum of $^{91}$Zr, which is well established experimentally and offers clean constraints on the interaction. The only unknown single-particle orbital in $^{91}$Zr, which is the neutron $h_{11/2}$, have been estimated to be around 3.5 MeV (it was placed at 3.5 MeV in Ref. [15]), see Sec. III C for further details. The calculated spectrum of $^{91}$Zr is shown in Fig. 3. A fair agreement with experiment is also found in $^{93}$Zr and $^{95}$Zr, as is shown in Figs. 4 and 5. It is worth mentioning that in $^{93}$Zr the low-lying state at 950 keV, which has been assigned $1/2^+$ in Ref. [1], is proposed to be rather a $9/2^+$ state in Refs. [22,23]. As was argued in Ref. [15], these states are found to be of seniority $\nu = 3$ nature, three $d_{5/2}$ neutrons being coupled to a $J^\pi = 5/2^+, 7/2^+, 9/2^+$ multiplet below 1 MeV. Indeed, the $9/2^+$ calculated here at 0.917 MeV has a $\nu(d^3_{5/2})$ configuration which supports the $9/2^+$ spin-parity assignment of Refs. [22,23].

The $^{97}$Zr nucleus has a pronounced single-particle structure and is fairly reproduced in the present SM calculation, see Fig. 6. We have listed the occupation numbers for its yrast states in Table I. It is seen that the ground state with $J^\pi = 1/2^+$ and the excited $3/2^+, 7/2^+$, and $11/2^-$ states can be considered as one-quasiparticle states built on the closed $^{96}$Zr core, while the $5/2^+$ is a one-hole state in the $^{98}$Zr core.

Let us discuss in more detail the evolution of $11/2^-$ states in subsequent Zr isotopes. We obtain that the $11/2^-$ level at 2.0 MeV in $^{91}$Zr is not a pure single-particle $h_{11/2}$ level,

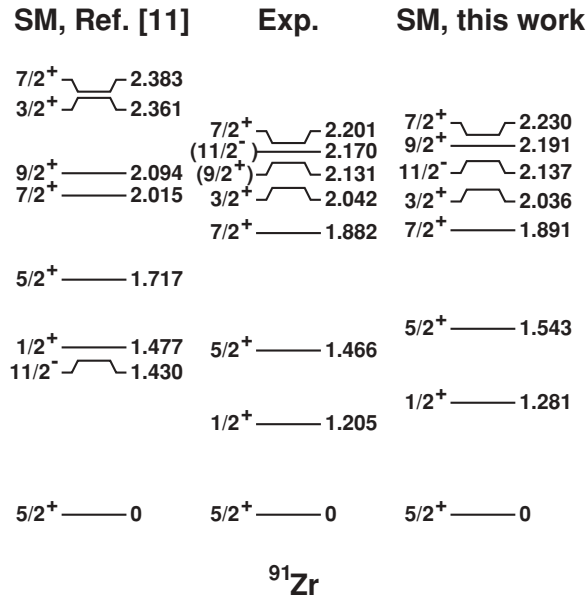


FIG. 3. Experimental low-lying spectra of $^{91}$Zr (center) compared with the SM calculations with the $^{78}$Ni core and the effective interaction obtained in this work (right) and the SM calculations from Ref. [15] with the $^{88}$Sr core (left).

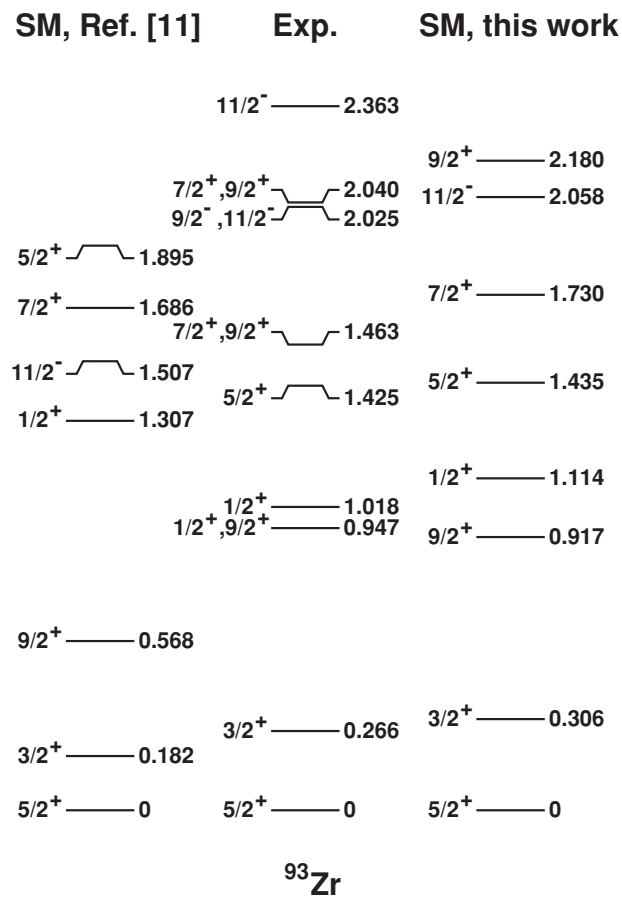


FIG. 4. Same as Fig. 3, but for $^{93}$Zr.

but it is calculated to have a dominant $\pi(p^1_{1/2}g^1_{9/2})\nu(d^1_{5/2})$ component (55%). The total number of neutrons in the $h_{11/2}$ orbital is calculated to be only 0.16. The spectroscopic factor for the first $11/2^-$ level was measured to be 0.37–0.53 depending on the reaction mechanism [24], and we obtain in our calculation a value of 0.377. A similar structure is found for $11/2^-$ in $^{93}$Zr, where the dominant configuration is the $\pi(p^1_{1/2}g^1_{9/2})\nu(d^3_{5/2})$; and in $^{95}$Zr, $\pi(p^1_{1/2}g^1_{9/2})\nu(d^5_{5/2})$. The total occupancies of the $h_{11/2}$ orbital in these nuclei are equal to 0.27 and 0.25, respectively. However, because of the $d_{5/2}$ shell closure in $^{97}$Zr, the calculated low-lying $11/2^-$ level acquires a single-particle nature. This result is contradictory to previous SM calculations [15], where the lowest calculated $11/2^-$ states were always predominantly based on the proton $g^1_{9/2}p^1_{1/2}$

TABLE I. Occupation numbers in $^{97}$Zr calculated in SM with a $^{78}$Ni core.

| $J^\pi$ | $f_{5/2}$ | $p_{3/2}$ | $p_{1/2}$ | $g_{9/2}$ | $d_{5/2}$ | $s_{1/2}$ | $g_{7/2}$ | $d_{3/2}$ | $h_{11/2}$ |
|---|---|---|---|---|---|---|---|---|---|
| $1/2^+$ | 5.66 | 3.78 | 1.84 | 0.71 | 5.54 | 0.96 | 0.15 | 0.17 | 0.16 |
| $3/2^+$ | 5.67 | 3.74 | 1.81 | 0.76 | 5.51 | 0.13 | 0.16 | 1.00 | 0.18 |
| $5/2^+$ | 5.63 | 3.82 | 1.82 | 0.71 | 4.73 | 1.69 | 0.18 | 0.19 | 0.18 |
| $7/2^+$ | 5.63 | 3.72 | 1.79 | 0.85 | 5.43 | 0.16 | 1.04 | 0.16 | 0.18 |
| $11/2^-$ | 5.71 | 3.76 | 1.81 | 0.69 | 5.65 | 0.11 | 0.10 | 0.14 | 0.98 |

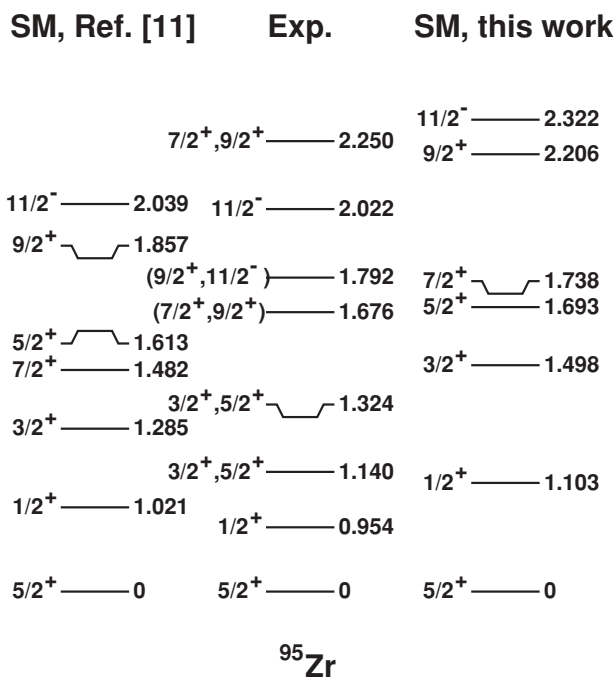


FIG. 5. Same as Fig. 3, but for $^{95}$Zr.

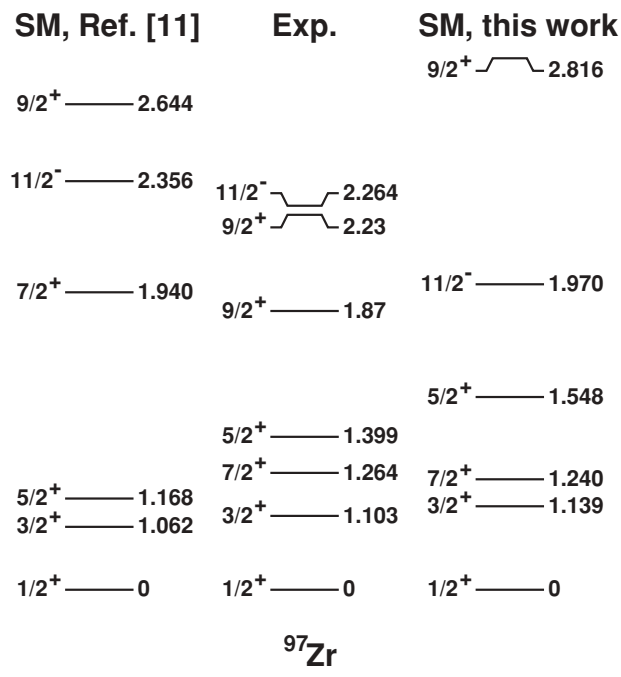


FIG. 6. Same as Fig. 3, but for $^{97}$Zr.

configuration. It can be seen from Fig. 1 that our interaction causes an increase of the gap between $p_{1/2}$ and $g_{9/2}$ levels with the filling of the $d_{5/2}$, $s_{1/2}$ orbitals. This explains why the $[\pi(g^1_{9/2}p^1_{1/2})\nu(s^1_{1/2})]_{11/2^-}$ coupling is no longer favored in our calculation for $^{97}$Zr. The fact that our SM calculations predict a $11/2^-$ level of a single-particle structure around 2 MeV in $^{97}$Zr is, however, in agreement with the experimental $\nu h_{11/2}$ level identification at 2263 keV from Ref. [25]. Future studies of the $^{97}$Zr nucleus with the inclusion of the recent data for high-spin states [26] will be done to better determine the evolution of the single-particle $h_{11/2}$ orbital along the chain [27].

### B. Even isotopes

The spectra of even zirconium isotopes compared with SM results from Ref. [15] are shown in Figs. 7–11. A nice description of the measured data is found for the yrast bands in all isotopes. Nevertheless, this is no longer the case for the $3^-$ states which deviate considerably from experimental data beginning with $^{94}$Zr. The experimental spectrum of $^{94}$Zr is of a vibrational nature, where the $3^-$ state can be interpreted as the one-octupole phonon. The $3^-$ very collective states may correspond to a more complex superposition of cross shell excitations out of the valence space of these calculations.

It is important to note that the overall agreement with the measured data is far more satisfying in the present case than the calculations in a reduced valence space with the effective interaction from Ref. [15]. Our calculations indicate the non-negligible importance of the proton orbitals $f_{5/2}$ and $p_{3/2}$, especially when it comes to the reproduction of the energies of the first excited $0^+$ states. The occupation numbers of $0^+_1$ and $0^+_2$ states are given in Table II. Taking as examples $^{94}$Zr and $^{96}$Zr, one sees that the first excited $0^+$ state is predicted at a much too high energy in the calculation of Ref. [15], while it is brought down to the correct energy position in our case.

TABLE II. Calculated occupation numbers in $^{90}$Zr–$^{98}$Zr for the ground and first excited $0^+$ states.

| $N$ | $J^\pi$ | $f_{5/2}$ | $p_{3/2}$ | $p_{1/2}$ | $g_{9/2}$ | $d_{5/2}$ | $s_{1/2}$ | $g_{7/2}$ | $d_{3/2}$ | $h_{11/2}$ |
|---|---|---|---|---|---|---|---|---|---|---|
| 50 | $0^+_1$ | 5.67 | 3.67 | 1.27 | 1.38 | – | – | – | – | – |
| | $0^+_2$ | 5.70 | 3.58 | 1.0 | 1.71 | – | – | – | – | – |
| 52 | $0^+_1$ | 5.62 | 3.56 | 1.30 | 1.50 | 1.62 | 0.06 | 0.11 | 0.09 | 0.11 |
| | $0^+_2$ | 5.67 | 3.39 | 1.22 | 1.69 | 1.67 | 0.05 | 0.09 | 0.09 | 0.09 |
| 54 | $0^+_1$ | 5.60 | 3.59 | 1.53 | 1.26 | 3.31 | 0.11 | 0.19 | 0.16 | 0.22 |
| | $0^+_2$ | 5.61 | 3.29 | 1.17 | 1.91 | 3.05 | 0.17 | 0.23 | 0.34 | 0.18 |
| 56 | $0^+_1$ | 5.64 | 3.68 | 1.76 | 0.90 | 5.26 | 0.12 | 0.17 | 0.16 | 0.27 |
| | $0^+_2$ | 5.43 | 3.31 | 1.13 | 2.11 | 4.10 | 0.63 | 0.45 | 0.49 | 0.32 |
| 58 | $0^+_1$ | 5.52 | 3.76 | 1.77 | 0.93 | 5.37 | 1.57 | 0.40 | 0.33 | 0.32 |
| | $0^+_2$ | 5.41 | 3.60 | 1.53 | 1.44 | 5.07 | 0.71 | 1.26 | 0.54 | 0.40 |

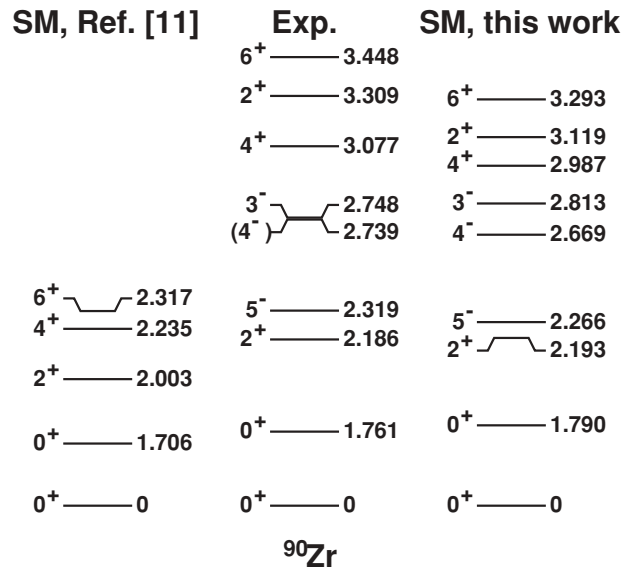


FIG. 7. Experimental low-lying spectra of even-even $^{90}$Zr (center) compared with the SM calculations of this work (right) and those from Ref. [15] (left).

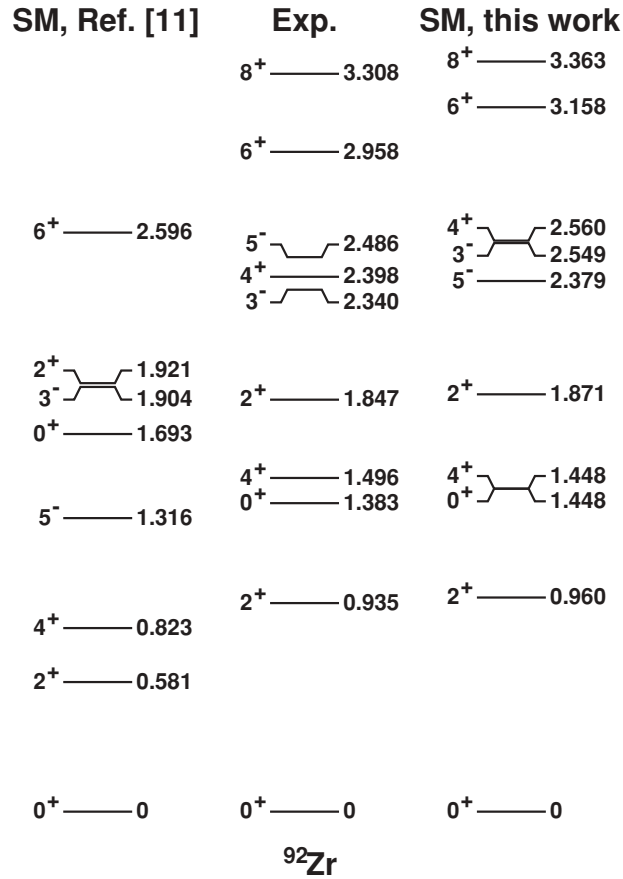


FIG. 8. Same as Fig.7, but for $^{92}$Zr.

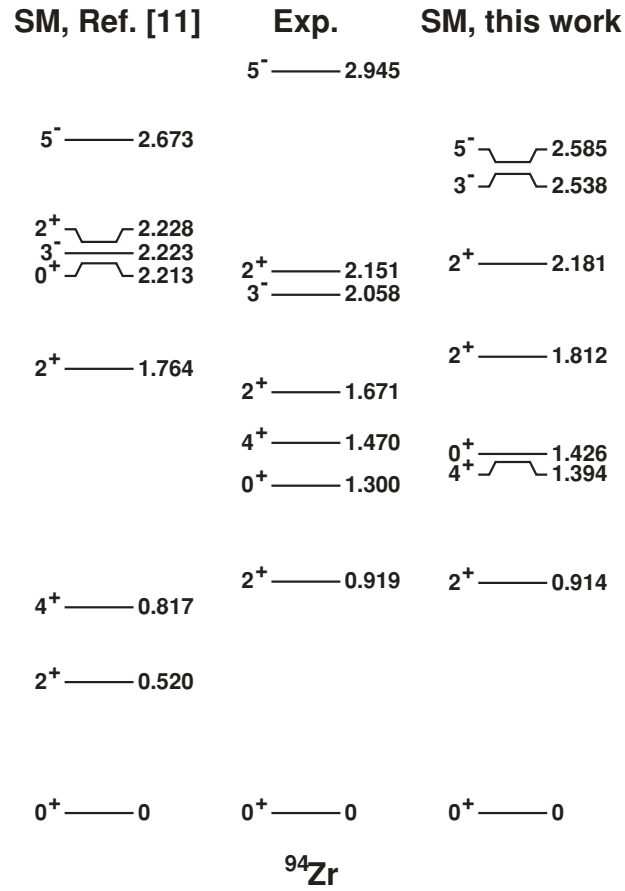


FIG. 9. Same as Fig. 7, but for $^{94}$Zr.

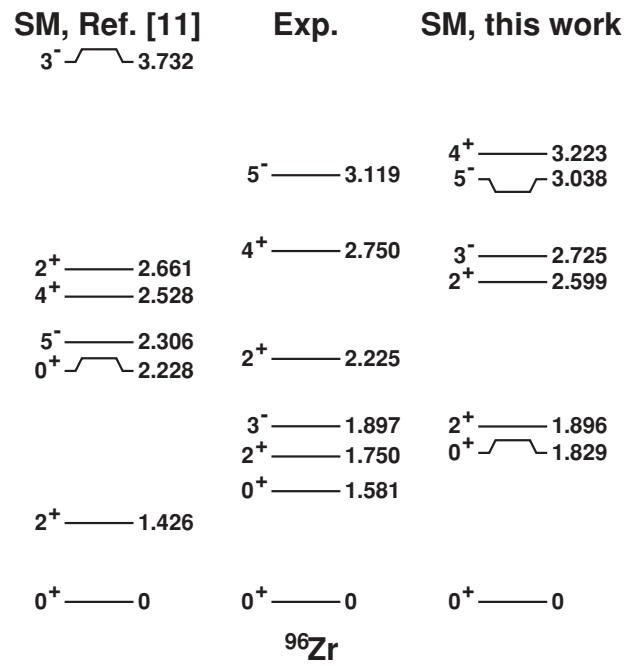


FIG. 10. Same as Fig. 7, but for $^{96}$Zr.

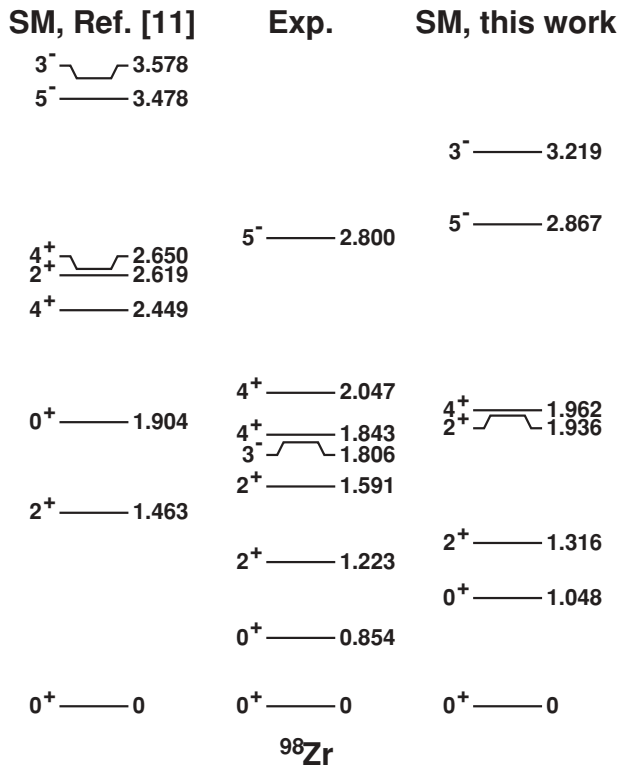


FIG. 11. Same as Fig. 7, but for $^{98}$Zr.

In these nuclei, our calculations indicate that first excited $0^+$ states correspond to 2p-2h proton excitations from the $p_{1/2}$ and $p_{3/2}$ to the $g_{9/2}$ orbital.

Another feature worth pointing out here is the subshell closure in $^{96}$Zr and $^{98}$Zr, due to the filling of the $d_{5/2}$ and $s_{1/2}$ orbitals, respectively. Clear signs for such a closure come from experimental data: the spacing between the ground state and the first $2^+$ state, almost equal for $N = 52$ and $N = 54$, is doubled for $N = 56$. This effect is accurately reproduced in our calculations, similar to the corresponding spacing in $^{98}$Zr (see Fig. 12).

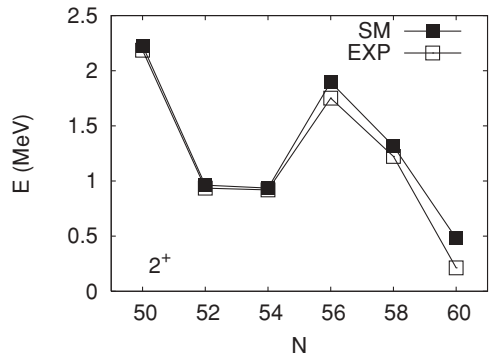


FIG. 12. Systematics of the experimental and theoretical first excited $2^+$ states along the zirconium chain.

### C. High-spin isomers

To better determine the position of the $\nu h_{11/2}$ level and to check the proton-neutron interaction between the $\nu h_{11/2}$ and the $\pi g_{9/2}$ orbitals, we looked for high-spin isomers observed in zirconium isotopes. The only two known cases, both assigned spin and parity $J^\pi = 17^-$, appear in $^{92}$Zr at an energy of 8041 keV [28] and in $^{98}$Zr at 6603 keV [29]. States with such a high spin in these nuclei can be generated by fully aligned $[\pi(g_{9/2}^2) \otimes \nu(g_{7/2}^1 h_{11/2}^1)]$ and $[\pi(g_{9/2} f_{5/2}^{-1}) \otimes \nu(h_{11/2}^2)]$ configurations, among which the former is more probable because of the strong attractive proton-neutron interaction between spin-orbit partners, which will lower the energy of such a level substantially. The (possibly) isomeric state in $^{92}$Zr is a good testing case because, thanks to the simple neutron structure of this nucleus (2 neutrons in $d_{5/2}$), a full diagonalization can be done in our valence space. We calculate the lowest $17^-$ state at the energy of 8310 keV, in a good agreement with experiment. As expected, the main component of the wave function (60%) of the state is the fully aligned $[\pi(g_{9/2})^2 \otimes \nu(g_{7/2}^1 h_{11/2}^1)]$ configuration. Turning to $^{98}$Zr, the additional six neutrons compared to $^{92}$Zr complicate the situation, since only a truncated calculation can be performed, and the final wave function is much more sensitive to the details of the monopole part of the effective interaction. We have done a 8p-8h calculation with respect to the $\nu s_{1/2}, \pi p_{1/2}$ closures, constraining additionally the maximal total occupancies of $g_{9/2}$ and $h_{11/2}$ orbitals to four. This way, we calculate the lowest $17^-$ state as a 5p-5h excitation at the energy of 6232 keV with the aligned $[\pi(g_{9/2})^2 \otimes \nu(g_{7/2}^1 h_{11/2}^1)]$ component as a dominant part of the wave function. In Table III, we list the total occupation numbers for the calculated $17^-$ states in $^{92,98}$Zr.

### D. Electric transition rates

To further test the quality of our SM wave functions, we have calculated several $E2$ electric transitions, which are listed in Table IV. First, we performed the calculations with the standard effective charges, i.e., $e_{\text{eff}}^\nu = 0.5$ and $e_{\text{eff}}^\pi = 1.5$. In this case in $^{90}$Zr, where only proton excitations are possible in our valence space, the electric transition is far too small as compared to the experiment. Thus proton excitations from the $pf$ shell to orbits above $\pi g_{9/2}$ and/or neutron excitation from the $\nu g_{9/2}$ orbital to higher shells may be necessary to account for the collectivity observed in $^{90}$Zr. This issue can only be clarified by studies performed in a valence space which is even larger than the present one, e.g., with the $^{56}$Ni inert core. Such calculations, however, are beyond the present computational possibilities. To account for the missing mixing of configurations, we therefore increased the effective charges to 1.8 for protons and 0.8 for neutrons. In Table IV,

TABLE III. Calculated structure of $17^-$ states in $^{92}$Zr and $^{98}$Zr.

| Nucleus | $f_{5/2}$ | $p_{3/2}$ | $p_{1/2}$ | $g_{9/2}$ | $d_{5/2}$ | $s_{1/2}$ | $g_{7/2}$ | $d_{3/2}$ | $h_{11/2}$ |
|---|---|---|---|---|---|---|---|---|---|
| $^{92}$Zr | 5.69 | 3.58 | 0.43 | 2.27 | 0.02 | 0.0 | 0.99 | 0.0 | 0.97 |
| $^{98}$Zr | 5.37 | 3.37 | 1.13 | 2.11 | 4.62 | 0.82 | 1.05 | 0.46 | 1.02 |

TABLE IV. Experimental $B(E2)$ transition rates in $e^2\,\mathrm{fm}^4$ vs SM results. SMI means calculations with standard effective charges: $e^{\nu}_{\mathrm{eff}} = 0.5$, $e^{\pi}_{\mathrm{eff}} = 1.5$; SMII stands for calculations with enhanced effective charges: $e^{\nu}_{\mathrm{eff}} = 0.8$, $e^{\pi}_{\mathrm{eff}} = 1.8$.

| $N$ | Transition | Exp | SMI | SMII |
|---|---|---|---|---|
| 50 | $B(E2;2^+_1 \to 0^+_1)$ | 122(8) | 84 | 121 |
| 52 | $B(E2;2^+_1 \to 0^+_1)$ | 166(12) | 78 | 151 |
| | $B(E2;2^+_1 \to 0^+_2)$ | 71(15) | 35 | 50 |
| | $B(E2;2^+_2 \to 0^+_1)$ | 84(10) | 72 | 100 |
| 54 | $B(E2;2^+_1 \to 0^+_1)$ | 132(28) | 58 | 120 |
| | $B(E2;2^+_1 \to 0^+_2)$ | 48(2) | 24 | 39 |
| | $B(E2;2^+_2 \to 0^+_1)$ | 198(18) | 84 | 140 |
| 56 | $B(E2;2^+_1 \to 0^+_1)$ | 110(44) | 57 | 113 |
| 58 | $B(E2;2^+_1 \to 0^+_1)$ | >6 | 40 | 70 |
| | $B(E2;2^+_1 \to 0^+_2)$ | >1 | 42 | 68 |

we compare the experimental values with calculations with standard effective charges (SMI) and with these slightly enhanced values (SMII). It is seen that in the SMII calculation, we reproduce the transitions rates rather well (note that in Ref. [15] much larger effective charges $e^{\nu}_{\mathrm{eff}} = 1.8$, $e^{\pi}_{\mathrm{eff}} = 1.5$ were needed to obtain agreement with data).

### E. Mixed symmetry states

The nuclides $^{92,94}$Zr belong to the $N = 52, 54$ isotone chains in which the so-called mixed symmetry (MS) states, which are proton-neutron isovector excitations of vibrational nature, have been observed [30–32]. These states are neither fully symmetric nor fully asymmetric with respect to the proton-neutron degree of freedom. Thus they are of special interest as a sensitive probe of the *pn* part of the residual interaction. The fundamental MS mode in nearly spherical nuclei is a $2^+$ excitation with a strong $M1$ transition to the one-phonon $2^+_1$ level and typically, a rather weak $E2$ transition to the ground state (see, e.g., Ref. [33] for a review). In this respect, an anomalous behavior for a MS state was observed in $^{94}$Zr [31]. The $2^+_2$ state at the energy 1667 keV depopulates by a strong $M1$ transition to the first excited $2^+$ state, suggesting the evidence of the mixed symmetry in this nucleus. However, an inversion of the $E2$ strengths takes place in $^{94}$Zr, i.e., the transition from the second excited (MS) $2^+_2$ state to the ground state is considerably larger than the one from the first excited $2^+$. Such an inversion has not been explained in the IBM-2 model with the F-spin symmetry, which is often used to describe mixed-symmetry states.

Our $B(E2)$ values, given in Table IV, are in fair agreement with experiment for the $2^+_i \to 0^+$ transitions. In particular, our calculation reproduces the inversion of $B(E2)$ strength, as we also calculate the transition from the second $2^+$ state to the ground state larger than from the first $2^+$ state. However, the calculated inversion is not as pronounced as experimentally observed. This might be due to the strong sensitivity of the $B(E2)$ values to small changes in the mixing between MS states. We note that in both $^{92}$Zr and $^{94}$Zr, the calculated structure of the first excited $2^+_1$ is the same, i.e., it corresponds predominantly to a neutron excitation (85% in both nuclei).

TABLE V. Experimental $B(M1)$ transition rates in $\mu^2_N$ vs SM results.

| $N$ | Transition | Exp | SM |
|---|---|---|---|
| 52 | $B(M1;2^+_2 \to 2^+_1)$ | 0.37(4) | 0.21 |
| | $B(M1;2^+_3 \to 2^+_1)$ | <0.024 | 0.06 |
| 54 | $B(M1;2^+_2 \to 2^+_1)$ | 0.33(5) | 0.10 |
| | $B(M1;2^+_3 \to 2^+_1)$ | 0.06(2) | 0.0 |

The $2^+_2$ state has a different structure in both nuclei. We find that in $^{94}$Zr, the main configurations in the wave function are $2^+_\nu \otimes 0^+_\pi$ (40%) and $0^+_\nu \otimes 2^+_\pi$ (35%), while in $^{92}$Zr the $0^+_\nu \otimes 2^+_\pi$ configuration dominates (51%) over the $2^+_\nu \otimes 0^+_\pi$ (25%). This inversion of proton and neutron components may explain the observed behavior of $E2$ transitions to the ground state.

In Table V, we have listed the calculated $B(M1)$ values for selected transitions. We have used the usual orbital $g$ factors ($g^p_l = 1.0$, $g^n_l = 0.0$) and a "standard" quenching factor 0.75 [34] of the spin $g$ factors. This allows us to reproduce the measured $g$ values, see Table VI, including the sign change between the first and second $2^+$ states. The calculated $B(M1)$ transitions are clearly enhanced for the second $2^+$ states in agreement with experimental data. In the calculations, the $0^+$ states contain 84% in $N = 52$ and 80% in $N = 54$ of seniority $\nu = 0$ configuration. The first excited $2^+$ states are dominated by the $\nu = 2$ component (87% and 76%, respectively). The second, mixed symmetry $2^+$ states are mainly formed of $\nu = 2, 4$, and 6 components: 60%, 18%, and 20% in $^{92}$Zr and 57%, 21%, and 18% in $^{94}$Zr. This complexity of wave functions shows that the calculated $2^+$ levels are not fully the symmetric and the MS one-phonon $2^+$ states.

### F. Shape transition

The experimental data in the zirconium chain exhibit a clear and smooth shape transition as a function of neutron number, from a spherical structure of $^{90}$Zr to an axially symmetric rotor in $^{102}$Zr. While the former can be well described in our calculations in the large model space with configuration mixing, similar calculations for $^{102}$Zr exceed the present computational possibilities. The shape transition is accompanied by a lowering of the first excited $0^+$ level, which moves from an energy of 1.5 MeV in $^{96}$Zr to only 0.2 MeV in $^{100}$Zr.

As demonstrated in Figs. 7–11, our SM calculations reproduce very nicely the low-lying spectra of even-even isotopes, including the subshell closures as well as the

TABLE VI. Experimental and theoretical values for $g$ factors in $N = 52, 54$ zirconium nuclei.

| $N$ | $g(J^\pi)$ | Exp | SM |
|---|---|---|---|
| 52 | $g(2^+_1)$ | −0.18(2) | −0.24 |
| | $g(2^+_2)$ | +0.76(50) | +0.79 |
| 54 | $g(2^+_1)$ | −0.32(2) | −0.31 |
| | $g(2^+_2)$ | +0.88(27) | +0.55 |

lowering of the first excited $0^+$ from $^{96}$Zr (1.8 MeV) to $^{98}$Zr (1.0 MeV). In Fig. 12, we compare the experimental and theoretical evolutions of the energy spacing between the ground state and the first $2^+$ state in Zr isotopes. For the calculations in $^{100}$Zr, however, we were forced to remove the $h_{11/2}$ orbital from the valence space. This restriction should not affect considerably the deformation of the ground state. The convergence of the calculated energies was achieved at 10p-10h level.

Figure 12 shows that the systematics of the $2^+$ levels changes rapidly at $N = 60$, where the energy of the calculated $2^+$ state is lowered from 1.31 MeV in $^{98}$Zr to only 0.48 MeV in $^{100}$Zr. This behavior has been already observed in the previous SM calculations of Federman and Pittel [5], however, within a smaller valence space. It seems to confirm the important role of the strong, attractive $g_{9/2}$-$g_{7/2}$ interaction. However, a proof of the intrinsic deformation in the laboratory frame can only be obtained from the $B(E2)$ value, which in experiment grows enormously, from 120 $e^2$ fm$^4$ for $N = 56$ to 2220 $e^2$ fm$^4$ for $N = 60$. Our SM calculations fail to produce such an enhancement: a value of only 180 $e^2$ fm$^4$ is obtained in the present calculation for $^{100}$Zr.

To understand this shortcoming, we have performed a set of explanatory studies. SM calculations of rotors in the $pf$ shell and in heavier nuclei [20] show that the Elliott's SU(3) scheme that is applicable to $sd$ nuclei can be there replaced by the approximate quasi-SU(3) [35] and pseudo-SU(3) [36] symmetries. One can use these findings to estimate the value of the quadrupole moment in any valence space. In our valence space, we may assume two pseudo-SU(3) blocks for the lower shells: a pseudo-$pf$ shell $[\nu(d_{5/2}, s_{1/2}, g_{7/2}, d_{3/2})]$ and a pseudo-$sd$ shell $[\pi(f_{5/2}, p_{3/2}, p_{1/2})]$. The $g_{9/2}$ and $h_{11/2}$ orbitals themselves do not induce quadrupole deformation. However, adding the proton $d_{5/2}$ orbital, quasi-SU(3) can operate for the upper proton shells. Similarly, to create a quasi-SU(3) block for neutrons, the $f_{7/2}$ orbital can be added to the $h_{11/2}$. One can then estimate the quadrupole moment of $^{100}$Zr in such a scheme.

The maximal value from the quadrupole moment is obtained if one considers six proton holes in the pseudo-$sd$ shell and six protons in the quasi-$gds$ shell in addition to six neutrons in the pseudo-$pf$ and four neutrons in the quasi-$fph$ shells. Adopting standard effective charges (1.5 for protons and 0.5 for neutrons), we obtain an $B(E2)$ value of $\sim$3300 $e^2$ fm$^4$, which is much larger than the observed one. Removing the quasi-SU(3) block for neutrons, the $B(E2)$ value is reduced to $\sim$2200 $e^2$ fm$^4$, which agrees well with experiment. Finally, taking into account only two pseudo-SU(3) blocks, thus the valence space considered in this work, we estimate a $B(E2)$ of only $\sim$700 $e^2$ fm$^4$. These results lead to the conclusion that the extension of the present valence space is necessary, but adding the $\pi d_{5/2}$ orbital may be already sufficient to account properly for the observed deformation in $^{100}$Zr.

## IV. SUMMARY AND PERSPECTIVES

We have performed large-scale shell model calculations for zirconium isotopes in a model space based on a $^{78}$Ni core [referred to as the $\nu(r4-h), \pi(r3-g)$ space], with a new effective interaction tailored for this valence space. Our calculations reproduce the low-spin spectroscopic data of $^{90-98}$Zr quite well. After estimating the position of the $h_{11/2}$ centroid in $^{91}$Zr at 3.5 MeV, the calculations do reproduce the isomeric states in $^{92,98}$Zr, which clearly involve excitations to this intruder orbital. We conclude that the interaction within this valence space can be used for calculations of other high-spin isomeric states in this mass region, which originate from deep proton holes coupled to neutron excitations to the $h_{11/2}$ intruder [37,38]. Such studies, in turn, should help to further constrain the location of the $h_{11/2}$ centroid and to tune the proton-neutron part of the effective interaction. We have probed as well the proton-neutron part of the interaction by calculating magnetic transitions in $^{92,94}$Zr, where the mixed-symmetry states, sensitive to the details of the $pn$ interaction, were observed. As a good qualitative description of these $B(M1)$ transition rates was achieved, the present interaction can be further explored in the investigations of MS states in $N = 52$ and $N = 54$ isotones. We have also reproduced qualitatively the $B(E2)$ transition rates; however, theoretical values calculated with standard effective charges $e^{\nu}_{\rm eff} = 0.5$, $e^{\pi}_{\rm eff} = 1.5$ are on average 40% smaller than the experimental ones. This defect can be cured by a readjustment of the effective charges: enhanced values $e^{\nu}_{\rm eff} = 0.8$, $e^{\pi}_{\rm eff} = 1.8$ allow us to get very good agreement with the data. Finally, we have shown that the deformation of the $^{100}$Zr ground state cannot be fully accounted in our adopted valence space, pointing to the need for a suitable enlargement together with an appropriate modification of the effective interactions. Such improvements are needed for a proper accounting of the deformation in $A \sim 100$ nuclei, and in particular for SM studies of the double-$\beta$ decays of $^{100}$Mo.

## ACKNOWLEDGMENTS

Discussions with E. Caurier, N. Pietralla, A. Poves, and W. Urban are greatfully acknowledged. This work has been supported by the state of Hesse within the Helmholtz International Center for FAIR (HIC for FAIR), by the DFG under Grant No. SFB 634 and by the Alliance Program of the Helmholtz Association (HA216/EMMI).

[1] http://www.nndc.bnl.gov/.
[2] H. Mach *et al.*, Nucl. Phys. **A523**, 197 (1991).
[3] H. Mach, M. Moszynski, R. L. Gill, G. Molnar, F. K. Wohn, J. A. Winger, and J. C. Hill, Phys. Rev. C **41**, 350 (1990).
[4] H. Mach *et al.*, Phys. Lett. **B230**, 21 (1989).
[5] P. Federman and S. Pittel, Phys. Rev. C **20**, 820 (1979).
[6] W. Urban *et al.*, Eur. Phys. J. A **16**, 11 (2003).
[7] W. Urban *et al.*, Eur. Phys. J. A **22**, 241 (2004).
[8] J. Skalski, S. Mizutori, and W. Nazarewicz, Nucl. Phys. **A617**, 282 (1997).
[9] J. Wood, K. Heyde, W. Nazarewicz, M. Huyse, and P. van Duppen, Phys. Rep. **215**, 101 (1992).

[10] G. Lalazissis and M. Sharma, arXiv:nucl-th/9501003v1.
[11] P. Bonche, H. Flocard, P. Heenen, S. Krieger, and M. Weiss, Nucl. Phys. **A443**, 39 (1985).
[12] S. Goriely, M. Samyn, and J. M. Pearson, Phys. Rev. C **75**, 064312 (2007).
[13] P. Möller, J. Nix, and K. Kratz, At. Data Nucl. Data Tables **66**, 131 (1997).
[14] J. García-Ramos, K. Heyde, R. Fossion, V. Hellemans, and S. De Baerdemacker, arXiv:nucl-th/0410045v2.
[15] A. Holt, T. Engeland, M. Hjorth-Jensen, and E. Osnes, Phys. Rev. C **61**, 064318 (2000).
[16] A. F. Lisetskiy, B. A. Brown, M. Horoi, and H. Grawe, Phys. Rev. C **70**, 044314 (2004).
[17] A. Gniady, E. Caurier, and F. Nowacki (unpublished).
[18] H. Grawe, K. Langanke, and G. Martíinez-Pinedo, Rep. Prog. Phys. **70**, 1525 (2007).
[19] T. Otsuka, M. Honma, T. Mizusaki, N. Shimizu, and Y. Utsuno, Prog. Part. Nucl. Phys. **47**, 319 (2001).
[20] E. Caurier, G. Martinez-Pinedo, F. Nowacki, A. Poves, and A. P. Zuker, Rev. Mod. Phys. **77**, 427 (2005).
[21] E. Caurier and F. Nowacki, Acta Phys. Pol. B **30**, 705 (1999).
[22] N. Fotiades *et al.*, Phys. Rev. C **65**, 044303 (2002).
[23] D. Pantelica *et al.*, Phys. Rev. C **72**, 024304 (2005).
[24] S. T. Thornton, D. E. Gustafson, J. L. C. Ford, K. S. Toth, and D. C. Hensley, Phys. Rev. C **13**, 1502 (1976).
[25] G. Lhersonneau *et al.*, Phys. Rev. C **54**, 1117 (1996).
[26] M. Matejska-Minda, B. Fornal, R. Broda, W. Królas, K. Mazurek, T. Pawłat, J. Wrzesiski, M. Carpenter, R. Janssens, and S. Zhu, Acta Phys. Pol. B **40**, 633 (2009).
[27] K. Sieja *et al.* (in preparation).
[28] G. Korschinek, M. Fenzl, H. Hick, A. Kreiner, W. Kutschera, E. Nolte, and H. Morinaga, Proceedings of the International Conference on Nuclear Structure, Tokyo, 1977.
[29] G. Simpson *et al.*, Phys. Rev. C **74**, 064308 (2006).
[30] C. Fransen *et al.*, Phys. Rev. C **71**, 054304 (2005).
[31] E. Elhami, J. N. Orce, S. Mukhopadhyay, S. N. Choudry, M. Scheck, M. T. McEllistrem, and S. W. Yates, Phys. Rev. C **75**, 011301(R) (2007).
[32] V. Werner *et al.*, Phys. Rev. C **78**, 031301(R) (2008).
[33] N. Pietralla, P. von Brentano, and A. Lisetskiy, Prog. Part. Nucl. Phys. **60**, 225 (2008).
[34] P. von Neumann-Cosel, A. Poves, J. Retamosa, and A. Richter, Phys. Lett. **B443**, 1 (1998).
[35] G. Martínez-Pinedo, A. P. Zuker, A. Poves, and E. Caurier, Phys. Rev. C **55**, 187 (1997).
[36] A. Arima, M. Harvey, and K. Shimuzi, Phys. Lett. **B30**, 517 (1969).
[37] T. Rzaca-Urban, K. Sieja, W. Urban, F. Nowacki, J. L. Durell, A. G. Smith, and I. Ahmad, Phys. Rev. C **79**, 024319 (2009).
[38] W. Urban *et al.*, Phys. Rev. C **79**, 044304 (2009).